

Variable range hopping theory for the nodal gap in strongly underdoped cuprate $\text{Bi}_2\text{Sr}_{2-x}\text{La}_x\text{CuO}_{6+\delta}$

Wei-Qiang Chen,¹ Jun-Qiu Zhang,¹ T. M. Rice,² and Fu-Chun Zhang^{3,4}

¹*Department of Physics, South University of Science and Technology of China, Shenzhen, China*

²*Institut für Theoretische Physik, ETH Zürich, CH-8093, Zürich, Switzerland*

³*Department of Physics, Zhejiang University, Hangzhou, China*

⁴*Collaborative Innovation Center of Advanced Microstructures, Nanjing, China*

Recent angle resolved photoemission spectroscopy (ARPES) experiments on strongly underdoped $\text{Bi}_2\text{Sr}_{2-x}\text{La}_x\text{CuO}_{6+\delta}$ cuprates have reported an unusual gap in the nodal direction. Transport experiments on these cuprates found variable range hopping behavior observed. These cuprates have both electron and hole doping which has led to proposals that this cuprate is analogous to a partially compensated semiconductors. The nodal gap then corresponds to the Efros-Schklovskii(ES) gap in such semiconductors. We calculate the doping dependence and temperature dependence of a ES gap model and find support for an Efros-Schklovskii model.

The parent compound of high temperature cuprate superconductor is a Mott insulator with antiferromagnetic(AFM) long range order¹. With doping of holes into the system, the AFM order is suppressed at first and finally vanishes at hole concentration $\sim 3\% - 5\%$. When the hole concentration exceeds a critical doping x_c , the system becomes superconducting. The evolution of the system with hole concentrations is one of the central issues in the field. Many experiments have been performed in the very underdoped and low temperature regime and various phenomena have been observed include spin glass, spin fluctuations, charge perturbations etc¹. One problem is that the impurity effect in this regime is strong because of the low carrier density and high impurity concentration (each impurity introduces one hole). This has led to debates about which phenomena are intrinsic or extrinsic due to the impurities. So it is timely to investigate the impurity effects in this regime. Recently, Yingying Peng et al. performed an ARPES and transport experiments on a series of $\text{Bi}_2\text{Sr}_{2-x}\text{La}_x\text{CuO}_{6+\delta}$ samples in this regime. They observed the variable range hopping behavior in the transport experiments and an energy gap along nodal direction in the ARPES spectra². By analogy to a partially compensated semiconductor, we attribute the energy gap to the soft gap opened in the impurity band due to the Coulomb interaction between the localized electrons. This indicates that the low energy physics in this material is dominated by impurity effects. Further experimental investigations of these materials will help to separate the extrinsic phenomena originating from impurity effects from the intrinsic phenomena.

In this paper, we examine the results of a recent series of ARPES and transport experiments on a series of $\text{Bi}_2\text{Sr}_{2-x}\text{La}_x\text{CuO}_{6+\delta}$ samples with low hole doping, lying just below the critical doping for the onset of superconductivity. These cuprates are unusual in that large concentrations of La donors were added, which are compensated by O acceptors. A series of samples were prepared with a large La donor concentration of $x = 0.84$ which were annealed in an O atmosphere. The result was

samples whose net carrier concentration, P , in the CuO_2 plane is $P < 0.10$. Superconductivity was observed in samples at the upper end of the doping range. Low hole doping in the planar CuO_2 can only be achieved in this way, when La donors and O acceptors are arranged in tightly bound neutral states leaving a small number of remaining holes in the more extended states in the CuO_2 planes. The values of the net carrier densities that result was estimated from a series of experiments, e.g resistivity, Hall coefficient and thermoelectric power. This procedure led to estimates of the critical concentration for superconductivity of $P = 0.1$. The spatial distribution of these different states is shown schematically in Fig 1. We will concentrate on the nonsuperconducting samples with net hole concentrations $P < 0.1$. We simulate the density of states with varying energy and temperature and compare with the results of the ARPES experiments.

In the ARPES experiments, one observes a peak-dip-hump structure. In the case with hole doping $0.03 < P < 0.1$, a gap is observed below the peak. The magnitude of the gap on the underlying Fermi surface is found to be k-dependent, minimal at the nodal direction and maximal in antinodal region. The gap value is reduced with increasing hole doping and vanishes at $P \sim 0.10$ where the system undergoes an insulator-superconductor transition. With increasing the temperature, the peak becomes weaker and weaker. Another very important phenomena observed in transport experiments on samples in this doping range, namely variable range hopping (VRH) behavior in the resistivity^{2,3}. VRH was proposed by Mott and has been well studied in semiconductors with localized impurity states forming impurity bands.⁴ In a partially compensated semiconductors, both acceptors and donors are present which form the acceptor bands and donor bands respectively. In a hole doped case, the donor bands are completely empty, while the acceptor bands are partially filled. At low temperatures, the hopping of holes can only happen between acceptor states which lie very close to the chemical potential. Because the localised acceptors are randomly distributed, acceptors with a small energy difference are well sepa-

rated. So the characteristic hopping length of holes will increase with decreasing temperature, leading to VRH. VRH makes the system an insulator though the acceptor band is only partially filled, leading to a resistivity which varies as $\rho_0 \exp[(T_0/T)^\alpha]$ with temperature. The exponent α is $1/3$ in 2D if there is a finite DOS at the Fermi level⁴. But Efros and Schklovskii (ES) pointed out later that because of the long range Coulomb interaction between the localised charges, a soft gap will open at chemical potential at zero temperature⁵. The direct consequence of the opening of ES gap is that the exponent becomes $\alpha = 1/2$ at very low temperature. With increasing temperature, the ES gap is filled and the exponent α will be reduced to $1/3$.

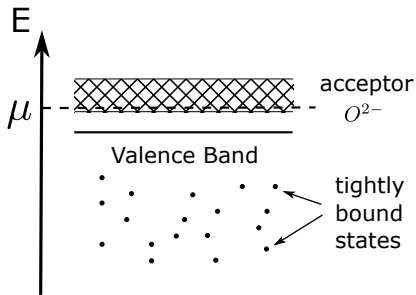


FIG. 1. A schematic figure of the band structure in lightly doped Mott insulators, $\text{Bi}_2\text{Sr}_{2-x}\text{La}_x\text{CuO}_{6+\delta}$ with both hole and electron dopants, similar to partially compensated semiconductors. The upper Hubbard band(not shown) acts as a conduction band, and the valence band is the lower Hubbard(or Zhang-Rice) singlet band. La^{3+} impurities form a donor band below the bottom of the conduction band, and the compensating O^{2-} ions form an acceptor band above the top of the valence band. Some holes and electrons form local bound states due to strong attraction between nearby La^{3+} and extra O^{2-} ions, with energies well below the top of the valence band. The chemical potential lies within the acceptor band due to the excess of holes.

In the experiments on $\text{Bi}_2\text{Sr}_{2-x}\text{La}_x\text{CuO}_{6+\delta}$, the transport data was fitted with the VRH form for both $\alpha = 1/3$ and $1/2$. But the fitting to an exponent $1/2$ is only good at low temperature, while the fitting to $1/3$ is good at much larger temperature region⁶. On one hand, this indicates a VRH physics in the $\text{Bi}_2\text{Sr}_{2-x}\text{La}_x\text{CuO}_{6+\delta}$ system. On the other hand, the exponent indicate a gap opens at low temperature which fills up at the temperature is raised. [Similar with the partially compensated semiconductor, the $\text{Bi}_2\text{Sr}_{2-x}\text{La}_x\text{CuO}_{6+\delta}$ material also has two kinds of dopants, the La^{3+} and the extra O^{2-} which introduce the electrons and holes respectively. So it is natural to make an analogy between the $\text{Bi}_2\text{Sr}_{2-x}\text{La}_x\text{CuO}_{6+\delta}$ and a partially compensate semiconductors, where the La^{3+} and extra O^{2-} play the role of donors and acceptors respectively.]

As discussed above, the VRH behavior in $\text{Bi}_2\text{Sr}_{2-x}\text{La}_x\text{CuO}_{6+\delta}$ material at low temperature indicate the opening of an ES gap. This gap should correspond to the gap observed in the experiments^{2,3}.

To investigate the properties of the ES gap, we follow earlier calculations^{5,7,8} and study the following classical Hamiltonian

$$H = \sum_i n_i \phi_i + \frac{V}{2} \sum_{i \neq j} \frac{n_i n_j}{r_{ij}}, \quad (1)$$

where i is the index of the centre of an impurity in the acceptor bands, ϕ_i is the energy of the corresponding localised state, $n_i = 0, 1$ is the occupation number of holes in the state, $V = e^2/4\pi\epsilon_r\epsilon_0 a$ is the coupling strength of the Coulomb repulsion between two holes, ϵ_r is the dielectric constant, r_{ij} is the distance between two impurities i and j . In our calculation, we assume that the impurities form a square lattice for simplicity. This approximation will not affect the result because only the states around the chemical potential are important, and those states are spatially separated and have randomly distributed energies as pointed out in ref.⁸. As mentioned above, most O acceptors form tightly bound neutral states with La donors and only a small fraction of extra O^{2-} show up in the acceptor band, i.e. the effective concentration n_a of O acceptors per Cu-site is much smaller than the nominal one $\delta = (x + P)/2 = 0.42 + P/2$. This leads to the uncertainty to estimate the charge carrier's filling ν_h in the acceptor band, which is defined by

$$\nu_h = P/n_a, \quad (2)$$

with P the concentration of doped holes in a Cu-oxide plane. Since $n_a < \delta$, we have $\nu_h > P/\delta$. While the precise relation between n_a and δ , hence the relation between ν_h and P , depends on the specific material, it is reasonable to assume ν_h and P are monotonic: a larger value of ν_h corresponds to a larger P in ARPES. In the calculations below, we consider three different values of ν_h : 0.88, 0.92, and 0.96.

First, we consider the density of states(DOS) at zero temperature of a 10×10 lattice with periodic boundary conditions. The DOS are calculated and averaged over 10^6 impurity configurations. In the calculations, the bandwidth of the acceptor band is chosen to be 200 meV, i.e. ϕ_i is generated randomly in the interval $[-100, 100]\text{meV}$. The Coulomb coupling strength V is chosen to 100meV which corresponds to $\epsilon_r \approx 38$. The electron distribution with lowest energy for each configuration is achieved with the procedure used in Ref. 7 and 8. At first, we generate an initial distribution of the holes randomly for a given impurity configuration. Then we apply the so-called μ -sub procedure. We calculated the single particle energy for each state with

$$E_i = \phi_i + \sum_{j \neq i} \frac{n_j}{r_{ij}}, \quad (3)$$

where r_{ij} is the shortest distance between two sites i and j . If E_i of highest occupied site is larger than E_i of the lowest empty site, we will move the hole from the highest occupied site to lowest empty site. Then we recalculate

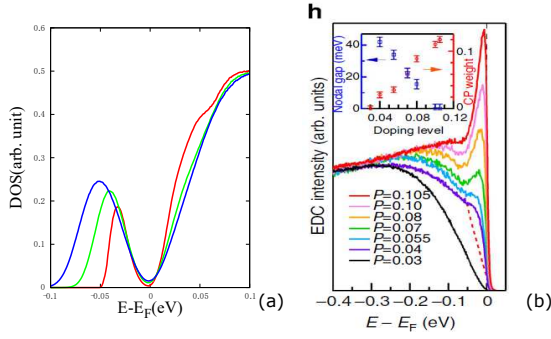


FIG. 2. (a) Calculated electron density of states (DOS) for various of filling factors of holes, ν_h in the impurity acceptor band: $\nu_h = 0.88$ (blue line), $\nu_h = 0.92$ (green lines), and $\nu_h = 0.94$ (red lines), respectively. (b) The ARPES data on energy distribution curve (EDC) for various hole dopings p , from fig. 3 in Ref. 2. The right panel in (b) shows only the occupied electron states which are observed in ARPES. Note that the position of the DOS peak shown in (a) shifts towards zero as ν_h increases, qualitatively consistent with the ARPES data, showing the peak position in EDC shifts towards zero as p hence ν_h increases.

E_i and do the check again and again until all E_i of occupied sites are less than any E_i of the empty sites.

In the next stage, we check the energy for a single hole, which hops with

$$E_{ji} = E_j - E_i - \frac{1}{r_{ij}}, \quad (4)$$

where i is an occupied site and j is an empty site. The hop will be performed if $E_{ji} < 0$. After each hop, we redo the μ -sub process and check all possible single hole hop until all E_{ji} are positive. Then we take the resulting hole distribution as one candidate ground state. After 5,000 iterations of the whole process for a given impurity configuration, we choose the one with lowest energy from all the candidates and choose it as the ground state for that impurity configuration.

With the single particle energy of the ground states, we can get the DOS by averaging over all the impurity configurations, the result is shown in fig. 2(a), where the DOS at $\nu_h = 0.88$ (blue line), 0.92 (green line) and 0.96 (red line) are depicted. To compare with the ARPES experiment, the DOS is presented in electron notation. It is obvious that a soft gap opened at the chemical potential for all of the three cases at low temperatures. The finite DOS at chemical potential at larger hole doping case may due to the finite size effect. The most important feature is that the peak position is shifted towards zero as the hole doping p increases, which is qualitatively consistent with the experimental result shown in fig. 2(b), which is extracted from fig. 3 in Ref. 2.

Then we study the DOS at finite temperature with the Monte Carlo technique used in ref.⁸. At first, we generate 10^4 random configurations of ϕ . For each configuration, we calculate the single particle energies from

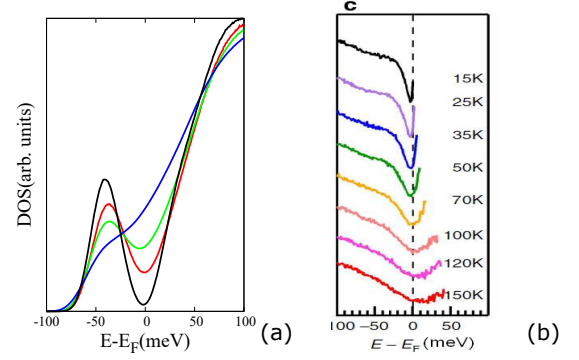


FIG. 3. (a) Calculated DOS at impurity acceptor band filling factor $\nu_h = 0.92$ at various temperatures: $k_B T = 0$ (black line), 6 meV (red line), 10 meV (green line), and 20 meV (blue line), respectively. (b) The ARPES result for energy distribution curve of at various temperatures, extract from fig. 4 in Ref. 2. See the text for a discussion of the qualitative agreement between the theory and experiment.

higher temperature to lower temperature with a standard Monte Carlo algorithm. At each temperature, we drop the first 10^4 hole configurations to remove the memory of higher temperature and keep the single particle energies for the next 10^5 hole configurations. By averaging over all the impurity configurations, we get the DOS at finite temperature. The result for $\nu_h = 0.92$ at temperatures $k_B T = 0$ (black line), 6 meV (red line), 10 meV (green line) and 20 meV (blue line) are depicted in fig. 3(a). With increasing temperature, the amplitude of the peak decreases while the DOS at the chemical potential increases leading to the closing of the ES gap. Note the position of the peaks shift only slightly to lower energy with increasing temperature. These results are consistent with the experiment shown in fig. 3(b) extracted from fig. 4 in Ref. 2.

Another feature of the ARPES experiments is the momentum dependence of the ES gap which is minimal at the nodal point and increases away from the nodal point. This momentum dependence may originate from the spatial distribution of the impurities which could be affected by various effects like clustering etc. at such high impurity densities. But in our model, we only consider the random distributed impurities because of the lack of information on the actual spatial distribution.

We have carried out simulations of the electron density of states for lightly doped cuprates with strong random potentials and compensated electron and hole dopings and compared them to the results of ARPES experiments on nonsuperconducting $\text{Bi}_2\text{Sr}_{2-x}\text{La}_x\text{CuO}_{6+\delta}$ samples whose transport properties show variable range hopping at low temperatures. The ARPES experiments measure only states occupied by electron with energies strictly below the chemical potential at low temperatures, extending to slightly above as T is raised. Our simulations show good agreement with the key features in the density and temperature dependence of the electron den-

sity of states and support the interpretation put forward by X. J. Zhou and collaborators of their experimental results.

Chen is partly supported by NSFC 11374135, and FC Zhang thanks NSFC 11274269, and National Basic Research Program of China (No. 2014CB921203).

ACKNOWLEDGMENTS

We thank X. J. Zhou for interesting discussions and allowing us to reuse the figures in their paper. WQ

-
- ¹ For a recent review see B. Keimer, S. A. Kivelson, M. R. Norman, S. Uchida, and J. Zaanen, *Nature* **518**, 179 (2015)
 - ² Yingying Peng, Jianqiao Meng, Daixiang Mou, Junfeng He, Lin Zhao, Yue Wu, Guodong Liu, Xiaoli Dong, Shaolong He, Jun Zhang, Xiaoyang Wang, Qinjun Peng, Zhimin Wang, Shenjin Zhang, Feng Yang, Chuangtian Chen, Zuyan Xu, T.K. Lee, X.J. Zhou, *Nat. Comms.* **4**, 2459 (2013).
 - ³ Z.-H. Pan, P. Richard, Y.-M. Xu, M. Neupane, P. Bishay, A. V. Fedorov, H. Luo, L. Fang, H.-H. Wen, Z. Wang, and H. Ding, *Phys. Rev. B* **79**, 092507 (2009).
 - ⁴ N. F. Mott, *J. Non-Cryst. Solids* **1**, 1 (1968).
 - ⁵ A. L. Efros and B.I. Shklovskii, *J. Phys. C* **8**, L49 (1975); B.I. Shklovskii and A. L. Efros, *Fiz. Tekh. Poluprovodn.* **14**, 825 (1980) [*Sov. Phys.-Semicond.* **14**, 487 (1980)].
 - ⁶ X. J. Zhou (private communication).
 - ⁷ S. D. Baranovskii, A. L. Efros, B. I. Gelmont, and B. I. Shklovskii, *J. Phys. C* **12**, 1869 (1979)
 - ⁸ J. H. Davies, P. A. Lee, T. M. Rice, *Phys. Rev. B* **29**, 4260 (1984)